

Broken Local Symmetry in Paraelectric BaTiO₃ Proved by Second Harmonic Generation

A. M. Pugachev,¹ V. I. Kovalevskii,¹ N. V. Surovtsev,¹ S. Kojima,² S. A. Prosandeev,^{3,4} I. P. Raevski,³ and S. I. Raevskaya³

¹*Institute of Automation and Electrometry, Russian Academy of Sciences, Novosibirsk, 630090, Russia*

²*Institute of Materials Science, University of Tsukuba, Tsukuba, Ibaraki 305-8573, Japan*

³*Research Institute of Physics and Physics Department, Southern Federal University, Rostov on Don, 344090, Russia*

⁴*Physics Department, University of Arkansas, Fayetteville, Arkansas 72701, USA*

(Received 30 December 2011; published 14 June 2012)

Precursor dynamics of a cubic to tetragonal ferroelectric phase transition in BaTiO₃ is studied by the accurate measurement of the second harmonic generation (SHG) integral intensities. A finite signal holds for the SHG integrated intensity above the ferroelectric Curie temperature $T_c = 403$ K. Above the Burns temperature $T_d \approx 580$ K, the power law with the exponent $\gamma = 1$ shows normal SHG nature originating from the hyper-Raman scattering by dynamical polar excitations, while, below T_d , a SHG signal from polar nanoregions becomes dominant with the larger exponent $\gamma = 2$. Such a crossover of the power law exponent near T_d is discussed on the basis of the effective Hamiltonian method and Monte Carlo simulation.

DOI: [10.1103/PhysRevLett.108.247601](https://doi.org/10.1103/PhysRevLett.108.247601)

PACS numbers: 77.84.-s, 77.80.Jk, 78.20.Bh, 78.35.+c

It has been established by Burns and Dacol that the temperature dependency of the refraction index in inhomogeneous lead-containing crystal $\text{PbMg}_{1/3}\text{Nb}_{2/3}\text{O}_3$ (PMN) experiences a deviation from a linear dependence starting from about $T_d = 620$ K, on cooling [1]. This evidence was interpreted as the appearance of polar nanoregions (PR), at $T = T_d$. Hyper-Raman studies showed the existence in PMN of specific soft modes, condensing at the Burns temperature, and nontrivial variation of the elastic signal [2]. A challenging question is if not only inhomogeneous crystals, but also more or less homogeneous ones can have PR. In this Letter, we study this question both experimentally and theoretically, by using the example of nominally pure BaTiO₃ (BTO).

Recently, Brillouin light scattering in the paraelectric phase of high quality BTO crystals revealed some acoustic anomalies and precursor dynamics [3]. These acoustic anomalies were correlated with the abnormal birefringence, piezoelectric effect, and deviation of the temperature dependence of dielectric permittivity from Curie-Weiss' law [4]. The deviation from a linear temperature dependence of the refractive index in pure BTO was also found in Ref. [5], but the most surprising result was the discovery of a finite integral second harmonic generation (SHG) intensity in the cubic paraelectric phase of BTO [6–9]. The reason for the appearance of such a signal in the centrosymmetric cubic phase of BTO has not been understood so far. In this study, we will explore this problem both experimentally and theoretically.

In our studies, we use BTO single crystals, ceramics, and powders. The BTO single crystals were grown by the top seeded solution growth method. The crystals obtained were cut to get (100)-oriented platelets, which were polished to optical quality. We will denote this sample as “sample 1.” In order to study the influence of the crystallite size, we made

BTO powder. For this purpose, we used the solid state reaction of the mixture of high purity BaCO₃ and TiO₂, at 1570 K for 3 hours. The obtained compact was crashed using a mortar and a pestle. Measurements of the size of particles in this powder, by using a Malvern Zetsizer Nano ZS spectrograph, revealed a bimodal distribution with the maxima at about 150 and 800 nm. This will be “sample 2.” With the aim to study the influence of the pressure on the SHG integral intensities, we pressed the powder by using a uniaxial pressure of 2×10^3 kg/cm², and we considered the resulting pellets as “sample 3.” The influence of the thermal treatment was studied in “sample 4,” by annealing sample 3 at 900 K for 2 hours. Finally, sample 5 presents BTO ceramics sintered at 1350 K for 3 hours in air and having a mean grain size of a few μm .

The SHG integral intensities were measured in the back-scattering geometry with the help of a Nd:YAG laser (wavelength equals 1064 nm). This is a diode-pumped solid state pulsed laser with the pulse duration of 0.6 ns, repetition rate of 1 kHz and average power of 100 mW. This choice is justified by the fact that the short-pulse irradiation allows one to reach a larger instant value of the power. It is known that the SHG intensity depends on the power quadratically. Thus, the choice of the short-pulse laser significantly improves the SHG performance. Notice that the probability of the crystal breakdown depends mostly on the average power, and, thus, our choice allows increasing the SHG signal without a danger to break the crystal down. The power of our laser is $I = 500 \times 10^3$ W, for one pulse. To our best knowledge, this value significantly exceeds the one in all previous measurements of the SHG integral intensity in BTO. With the use of the quadratic dependence of the SHG intensity on the power, we estimate that our SHG signal is 2500–10 000 times stronger than in all previous studies. Another problem is the noise.

We avoided this problem by the averaging of the result, at each given temperature, over the pulses. At first, the averaging was performed over 500 pulses that correspond to the time interval equal to 0.5 s. Then, the result was further averaged over 1000 such bunches. The square deviation of the results was not larger than the size of a symbol in our plots and, in the maximum, does not exceed 10% at $T > 900$ K. In order to take into account the secondary effects, we, first, looked for luminescence and, second, for thermal (Planck) irradiation. In all cases, we did not find any valuable luminescence, which was always below the noise signal, but we did find the Planck irradiation, at least, above 800 K. Notice that the thermal irradiation does not depend on the frequency that much as the SHG intensity. We took advantage of this circumstance and subtracted the average of the two signals, at 530 nm and 534 nm, corresponding to the thermal irradiation, from the main sharp signal detected at 532 nm. All the foregoing details allowed us to measure the SHG integral intensities in the temperature interval significantly exceeding the previous studies and reaching 1000 K, in the maximum. The measurements have been carried out in the heating mode. It is worth noting that during the subsequent cooling from temperatures exceeding 600 K we have not registered any valuable hysteresis. However, when the temperature in the heating run did not exceed 100–150 K above T_c , during the subsequent cooling, we did observe a hysteresis of several Kelvins in accord with Ref. [9].

For all studied samples, the temperature dependence of the normalized SHG signal $I_{2\omega}^{\text{norm}} = I_{2\omega}(T)/I_{2\omega}(300 \text{ K})$ is presented in Fig. 1. Here, $I_{2\omega}(T)$ and $I_{2\omega}(300 \text{ K})$ are the

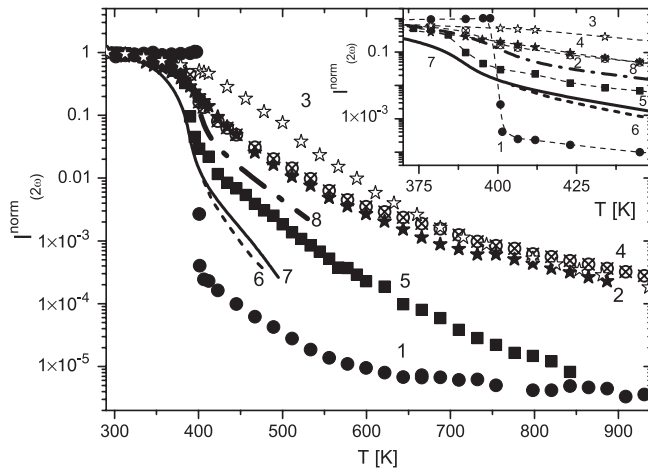


FIG. 1. Temperature dependences of the normalized SHG signal $I_{2\omega}^{\text{norm}} = I_{2\omega}(T)/I_{2\omega}(300 \text{ K})$ for the BTO samples studied: (1) single crystal, (2) powder, (3) pressed powder, (4) pressed and annealed powder, (5) ceramics (see text for details). Similar dependences were observed previously for BTO flux-grown crystals (curve 6 [8] and curve 7 [9]), as well as for BTO powder with mean particle size of $0.5 \mu\text{m}$ [9] (curve 8). The inset highlights the temperature range near T_c .

integral intensities of SHG at the current temperature and 300 K, correspondingly. We put in the same plot some literature data. In Refs. [8,9], SHG intensities were measured for BTO crystals grown by Remeika method. Powder BTO samples were used in Ref. [9]. Unfortunately, Ref. [8] does not contain any information about the magnitude of the signal at room temperature. We normalized these data using the data of Ref. [9] for a single crystal. One can see that, in all cases, the SHG integral intensities gradually decrease at temperature increase. The smallest magnitudes were detected in sample 1, which presents a single crystal. At the phase transition point, the SHG intensity has a discontinuity, because of the appearance of the polarization. Above T_c , BTO ceramics has a larger SHG intensity than in the crystals, but smaller than in powders. The increase of the SHG intensity in ceramics can be related to the high level of defects in the crystallite interfaces. The further increase of the SHG intensities in BTO powder can be explained by a larger amount of defects at the surface of the crystallites due to a smaller particle size and a lower coherence of the interfaces of particles as compared to grain boundaries in ceramics. In the pressed powder, SHG increases substantially and, at the same time, the $I_{2\omega}^{\text{norm}}(T)$ anomaly, at $T = T_c$, diffuses strongly (Fig. 1, curve 3). After annealing at 900 K for 2 hours, both the $I_{2\omega}^{\text{norm}}$ values and $I_{2\omega}^{\text{norm}}(T)$ anomaly at T_c restore (Fig. 1, curve 4). This fact can find its explanation if one assumes that the thermal treatment releases strains and cures the defectness. These results hint that the strains, surfaces, and defects are somehow related to the SHG signals in the paraelectric BTO. Similar conclusions were made in [10], when studying potassium tantalate with Li. The next challenge is finding the relation between the defects and SHG integral intensity.

SHG is a nonlinear optical effect resulting from a nonlinear dependence of the electric polarization on the electric field. The second harmonic is the polarization at the doubled frequency, the appearance of which results from the product of two components of the field generated at frequency ω ,

$$P_i(2\omega) = \beta_{ijk} E_j(\omega) E_k(\omega), \quad (1)$$

where β_{ijk} is the tensor of the nonlinear polarizability. The theory predicts that SHG integral intensity in ferroelectrics is proportional to the spontaneous polarization and to the third power of the first harmonic [11]. However, BTO, above the ferroelectric phase transition temperature T_c , is not ferroelectric, and the spontaneous polarization at zero bias field is absent. Thus, the reason for the SHG signal in the paraelectric phase of BTO is different.

Let us focus on the local inhomogeneity of the crystal structure of BTO. Such inhomogeneity can produce local random electric fields h_l , which contribute to the nonlinear polarizability via the hyper-Raman scattering [12],

$$\beta_{ijk} = \alpha_{ijkl} \sum G_{ll'} h_{l'}, \quad (2)$$

where G is the local linear polarizability tensor and α is the tensor responsible for hyper-Raman scattering. For the BTO lattice, this formula means, in particular, that the random field is produced by the point or extended defects. Light can, then, be scattered by these random fields. However, such an effect must be rather weak, because of the very small size of the defects and their small concentration in the nominally pure BTO.

Another effect is known in quantum paraelectrics: one can take into account the fact that a polar vibration fluctuation, enhanced by zero-point vibrations, can be pinned by lone impurities and this local polar mode can scatter the polarization second-harmonic wave [13]. This mechanism was shown to work properly in quantum paraelectrics like SrTiO_3 and KTaO_3 , at very low temperatures.

BTO is a classic soft-mode ferroelectric [14], but the story of the phase transition in BTO started, historically, from the Mason and Matthias order-disorder model [15], which related the ferroelectric phase transition to the ordering of the Ti displacements in a six-well potential (see also experiment [16]). Girshberg and Yacoby developed a combined model [17], and, finally, Pirc and Blinc [18] argued that the real story should include an eight-site model (instead of the six-site Mason-Matthias model), and should include the soft mode variables, which are coupled bilinearly to the local Ti off-centerings. Recently, experimental results and first-principles-based molecular dynamics simulations have confirmed the existence of the Ti off-centerings above T_c in BTO [19].

In our opinion, PR in BTO can be related to local defects pinning the off-center Ti displacements. In order to find the SHG integral intensity triggered by such PR, we expand the polarizability tensor over the local polarization P_l related to the l th atomic center,

$$\beta_{ijk} = \sum C_{ijkl} P_l. \quad (3)$$

Here, C_{ijkl} are the coefficients of this expansion. The SHG integral intensity can be found as the magnitude of the scattering of the second harmonic by these polar modes,

$$\langle \beta_{ijk} \beta_{lmn} \rangle = C_{ijkk'} C_{lmnn'} \langle P_{k'} P_{n'} \rangle. \quad (4)$$

Let us divide the polarization into two parts. The first part is related to the polarization induced by the local random field $h(l)$

$$P_l^i = G_{ll'} h_{l'} \quad (5)$$

and the other is due to the polar soft mode, in the absence of the random field. If one substitutes Eq. (5) to Eq. (4), the induced contribution will be proportional to the square of the dielectric susceptibility,

$$I^i \sim \chi^2 \sim \frac{C}{(T - T_c)^{\gamma^i}}. \quad (6)$$

In contrast to this, the soft-mode part will be proportional to the first power of the dielectric susceptibility, as this follows from Eq. (4) (because the dielectric susceptibility is proportional to the polarization-polarization correlator):

$$I^p \sim \chi \sim \frac{1}{(T - T_c)^{\gamma^p}}. \quad (7)$$

If one assumes that the Landau critical exponents are valid [14], then $\gamma^i = 2 \times \gamma(\text{Landau}) = 2$ and $\gamma^p = \gamma(\text{Landau}) = 1$. The importance of these two different contributions to the SHG intensity can vary in different temperature intervals. For example, at high temperatures, the static (defect) part should be small compared to the dynamical part. In this case, one can expect the exponent equal to 1 or close to it. At lower temperatures, where the Ti off-centerings are pinned by defects, one can expect the gain of the intensity related to the induced contribution, and the proposed exponent, in this case, should be close to 2. In order to theoretically find the pinning temperature, one can employ an analog of the Edwards-Anderson parameter,

$$q = \langle (\langle P_i - \langle P \rangle) \rangle^2 \rangle. \quad (8)$$

Here, P_i is the local polarization around site i , and $\langle P \rangle$ is the average over the sample polarization. The first averaging in (8) is over time (or, in the Monte Carlo approach, over the Monte Carlo steps), and the next averaging is over the lattice sites. To consider a realistic microscopic model, we employed the effective Hamiltonian approach [20], which includes the local ferroelectric soft modes and inhomogeneous and homogeneous strain tensors. We apply this Hamiltonian to calculate the temperature-related variables in the manner, which is close to Ref. [21], but differs from this approach by introducing the random fields. Specifically, we employ a periodic $12 \times 12 \times 12$ barium titanate supercell. With the help of a random number generator, we distributed a small random field over the one hundredth of the lattice sites selected randomly. The directions and magnitudes of the random fields were selected also randomly. The maximal magnitude of the random field was 10^6 V/m. Fig. 2 presents the log-log plot of the temperature dependency of the inverse q magnitudes, as calculated in the framework of this effective Hamiltonian model. One can see that $\log_{10}(q^{-1})$ has several linear portions, which change their inclination on cooling, first, from a small angle to a larger one, and, then, from this large inclination, in two steps, to smaller ones. The first (high-temperature) change can manifest the pinning-depinning local transformation, while the next ones might be responsible for the change of the PR growth process from the ferroelectric fluctuation kind to the limited growth (because of further PR, having different directions of the quenched internal field, touching).

Generally, SHG can manifest two different effects, intrinsic and extrinsic. In the ceramics and powder, the effect considered is definitely extrinsic, as this is seen from the enhanced magnitude of the intensity. In some previous studies of BTO single crystals [6–9], the SHG intensity

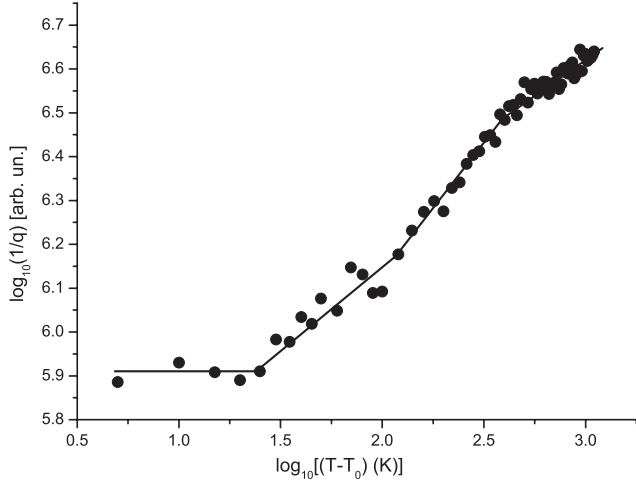


FIG. 2. Temperature dependence of the inverse Edwards-Anderson parameter, in the log-log scale, obtained in our Monte Carlo simulation, at the defect concentration equal to 1%, maximal magnitude of the electric field equal to 10^6 V/m, and $T_0 = 400$ K. Lines are guides for the eye.

was also high, and significantly exceeded the values obtained by us for sample 1 that can also manifest some extrinsic effect. Let us focus on the data obtained for sample 1, to analyze the temperature trend of this SHG intensity. Fig. 3 presents the inverse SHG integral intensity for sample 1, in a log-log scale. One can see that this dependence can be described by four consequent portions of the power law having different exponents γ . The low temperature portion has the exponent close to zero, the adjacent portion from the high temperature side has an exponent of 1.2. The two next portions from the high temperature side have the exponents close to 2 and 1, correspondingly. We relate the exponent equal to 2, in the middle part, to the scattering of the polarization second

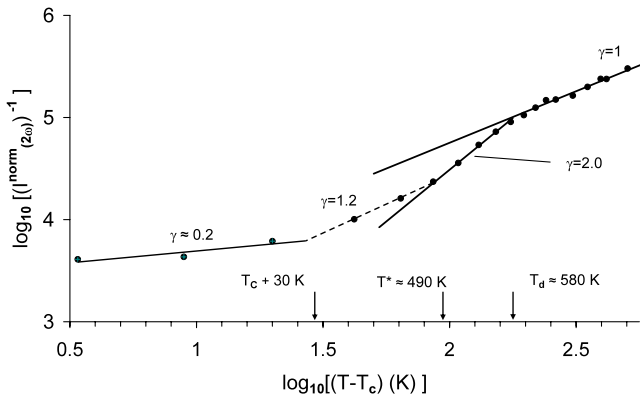


FIG. 3 (color online). Dependency of the normalized SHG signal for BTO melt-grown crystal (sample 1) on the reduced temperature $T-T_c$ plotted in the double-logarithmic scale. Points are experimental data, and lines are the mean-square fits by a power law.

harmonic by PR. It is interesting that this kind of behavior is inherent also to the dielectric permittivity in relaxors and to the correlation function in the percolation theory ($\gamma = 1.7$) [22]. The smaller exponent, which is close to 1 and corresponds to the highest temperatures in the plot, is inherent to the ordinary mean-field approximation [14], and it can be explained by the dynamical scattering of light by polar phonon excitations. The switch between these exponents happens in some interval around the Burn's temperature $T_d = 580$ K. It is interesting that, in the same temperature interval, Dul'kin *et al.* [23] found a thermally stimulated acoustic emission, which can also be interpreted as an evidence of the Burn's temperature. This puts some arguments in favor of the thought that the Burn's temperature manifests a critical phenomenon. The portion having the exponent equal to 1.2 and lying below $T^* \approx 490$ K can be interpreted now as the PR limited growth inherent to liquids. The existence of this portion is reminiscent to the similar portion found in our calculations. We should mention that the positions of the temperature anomalies found in our calculation do not coincide with experiment, but this is not surprising, because these positions depend on the concentration of the defects and the maximum electric field magnitude. At the same time, we have a qualitative agreement between the stages of the growth of PR's in the theory and experiment, from the Burn's temperature, on cooling, to T^* , and, then, to T_c . Temperature T^* has been established also in PMN, in several independent experimental studies [24,25]. We interpret this temperature as the manifestation of the change of the growth mechanism from the Ornstein-Cernike type to the quasistatic limited growth. It is remarkable that the temperature stimulated acoustic emission in BTO has an anomaly at a close temperature $T^* \approx 500$ K, [23].

The portion, which is the closest to T_c , presents the behavior inherent to quantum paraelectrics, which normally show some saturated region below the saturation temperature [13]. Large polar clusters were observed in BTO crystals by Brillouin light scattering [4] in the same temperature interval $T_c + (30-40)$ K. The conception of the broken symmetry as a precursor phenomenon has been also developed in [26]. These slow-dynamic clusters may appear due to pretransitional local dynamics, e.g., ferroelectric fluctuations. Thus, the SHG signal can, in principle, appear in this region owing to the scattering of the second harmonic by these slow fluctuations. Formation of surface ferroelectric domains prior to the ferroelectric transition in bulk is also a possible scenario. This kind of dependence has also been noticed, when treating the Ti off-centering temperature behavior in BTO, with the help of a spin-like variable [17,18]. It is instructive to realize that the slow polarization fluctuations in PR play the same role in BTO as the zero point quantum vibrations in the low temperature phase of quantum paraelectrics.

In conclusion, the broken local symmetry of a cubic BaTiO₃ has been studied by the accurate measurement of SHG. The power law of the SHG integrated intensity showed the crossover, near the Burns's temperature $T_d \approx 580$ K, from the exponent $\gamma = 1$, owing to the scattering by polarization fluctuations, into the larger exponent $\gamma = 2$, owing to the scattering by polar nanoregions having strongly correlated polar displacements. These different mechanisms have been confirmed by the theoretical consideration based on the effective Hamiltonian method and Monte Carlo simulation assuming the existence in the sample of the random fields. It is interesting to consider the SHG integral intensity in a nonferroelectric media as a nontrivial order parameter in relaxors characterizing PR. From this point of view, our result may be generalized for all relaxors.

The authors are grateful to E. A. Turnina, Ural Federal University, for the measurement of the size of BTO powder particles, and to Dr. L. N. Korotkov, Voronezh State Technical University, for providing a BTO ceramic sample. The work was partially supported by the Russian Foundation for Basic Research (Project No. 09-02-00451-a) and Foundation for Interdisciplinary Studies of the Syberian Branch of the Russian Academy of Sciences (Project No. 101). S.P. appreciates ONR Grants No. N00014-08-1-0915 and N00014-11-1-0384.

-
- [1] G. Burns and F. H. Dacol, *Phys. Rev. B* **28**, 2527 (1983).
 - [2] A. Al-Zein, J. Hlinka, J. Rouquette, and B. Hehlen, *Phys. Rev. Lett.* **105**, 017601 (2010); A. Al-Zein, J. Hlinka, J. Rouquette, A. Kania, and B. Hehlen, *J. Appl. Phys.* **109**, 124114 (2011).
 - [3] J.-H. Ko, T. H. Kim, K. Roleder, D. Rytz, and S. Kojima, *Phys. Rev. B* **84**, 094123 (2011).
 - [4] M. Takagi and T. Ishidate, *Solid State Commun.* **113**, 423 (2000); K. Rusek, J. Kruczek, K. Szot, D. Rytz, M. Górný, and K. Roleder, *Ferroelectrics* **375**, 165 (2008).
 - [5] G. Burns and F. G. Dacol, *Solid State Commun.* **42**, 9 (1982).
 - [6] V. S. Gorelik, O. P. Maksimov, G. G. Mitin, and M. M. Sushchinskii, *Sov. Phys. Solid State* **15**, 1133 (1973).
 - [7] J. P. Dougherty and S. K. Kurtz, *J. Appl. Cryst.* **9**, 145 (1976).
 - [8] G. V. Liberts and V. Ya. Fritsberg, *Phys. Status Solidi A* **67**, K81 (1981).
 - [9] G. R. Fox, J. K. Jamamoto, D. V. Miller, L. E. Cross, and S. K. Kurtz, *Mater. Lett.* **9**, 284 (1990).
 - [10] H. Yokota, Y. Uesu, C. Malibert, and J.-M. Kiat, *Phys. Rev. B* **75**, 184113 (2007).
 - [11] Y. Ishibashi, *J. Korean Phys. Soc.* **32**, S407 (1998).
 - [12] V. E. Kravtsov, V. M. Agranovich, and K. I. Grigorishin, *Phys. Rev. B* **44**, 4931 (1991).
 - [13] W. Prusseit-Elffroth and F. Schwabl, *Appl. Phys. A* **51**, 361 (1990).
 - [14] L. D. Landau and E. M. Lifshitz, *Statistical Physics* (Butterworth-Heinemann, London, 1980), Vol. 5, Part 1.
 - [15] W. P. Mason and B. T. Matthias, *Phys. Rev.* **74**, 1622 (1948).
 - [16] R. Comes, M. Lambert, and A. Guinier, *Acta Crystallogr. A* **26**, 244 (1970).
 - [17] Y. Girschberg and Y. Yacoby, *J. Phys.: Condens. Matter* **13**, 8817 (2001).
 - [18] R. Pirc and R. Blinc, *Phys. Rev. B* **70**, 134107 (2004).
 - [19] J. Hlinka, T. Ostapchuk, D. Nuzhnyy, J. Petzelt, P. Kuzel, C. Kadlec, P. Vanek, I. Ponomareva, and L. Bellaiche, *Phys. Rev. Lett.* **101**, 167402 (2008).
 - [20] W. Zhong, D. Vanderbilt, and K. M. Rabe, *Phys. Rev. Lett.* **73**, 1861 (1994); *Phys. Rev. B* **52**, 6301 (1995).
 - [21] L. Walizer, S. Lisenkov, and L. Bellaiche, *Phys. Rev. B* **73**, 144105 (2006).
 - [22] D. Stauffer and A. Aharony, *Introduction to Percolation Theory* (Taylor & Francis, London, 1994).
 - [23] E. Dul'kin, J. Petzelt, S. Kamba, E. Mojaev, and M. Roth, *Appl. Phys. Lett.* **97**, 032903 (2010).
 - [24] O. Svitelskiy, J. Toulouse, G. Yong, and Z.-G. Ye, *Phys. Rev. B* **68**, 104107 (2003).
 - [25] B. Dkhil, P. Gemeiner, A. Al-Barakaty, L. Bellaiche, E. Dul'kin, E. Mojaev, and M. Roth, *Phys. Rev. B* **80**, 064103 (2009).
 - [26] A. Bussmann-Holder, H. Beige, and G. Völkel, *Phys. Rev. B* **79**, 184111 (2009).